Progress In Electromagnetics Research, PIER 103, 241–257, 2010

SPICE MODELS FOR RADIATED AND CONDUCTED SUSCEPTIBILITY ANALYSES OF MULTICONDUCTOR SHIELDED CABLES

H. Xie, J. Wang, R. Fan, and Y. Liu †

Department of Engineering Physics
Tsinghua University
Beijing 100084, China

Abstract—This paper presents SPICE models to analyze the radiated and conducted susceptibilities of multiconductor shielded cables in the time and frequency domains. These models, which can be used directly in the time and frequency domains, take into account the presence of both the transfer impedance and admittance, and allow the transient analysis when the termination is nonlinear or time-varying. The radiated and conducted susceptibilities are studied by using an incident plane-wave electromagnetic field and an injection current on the cable shield as the source, respectively. Results obtained by these models are in good agreement with those obtained by other methods.

1. INTRODUCTION

Shielded cables are usually used in wired communication systems to protect signal transmission from external interference. Multiconductor shielded cables are more appealing compared with coaxial shielded cables due to the capability to transmit differential signals. Nevertheless, there exists coupling between the exterior and interior of the shield due to the imperfect nature of the shield. Consequently, prediction of the susceptibility of multiconductor shielded cables will be helpful for the optimization of system design.

SPICE equivalent circuit models for multiconductor transmission lines without shields have drawn much attention, and lots of researches have done on them and their applications [1–9]. Recently, some interest has been addressed to the development of SPICE models for the susceptibility analysis of shielded cables. SPICE models to analyze the

Corresponding author: H. Xie (xiehy05@mails.tsinghua.edu.cn).
† J. Wang and R. Fan are also with the Northwest Institute of Nuclear Technology, P. O. Box 69-1, Xi'an, Shaanxi 710024, China.

conducted immunity of both lossless and lossy coaxial cables have been presented in [10], and the inverse Fourier transform (IFT) is needed to get the time domain results. Then, some SPICE models have been proposed for the time and frequency domain analyses of bulk current injection test on lossless shielded cables [11, 12]. However, the radiated immunity can not be directly analyzed with these models. Recently, some circuit models have been developed to analyze the conducted and radiated immunity of shielded cables [13], and the IFT is required for the models to obtain the time domain results. After then, some lossless models have been proposed to analyze the radiated and conducted susceptibilities of coaxial shielded cables [14]. These models can be employed directly in the time and frequency domains and take into account both the transfer impedance and admittance of the shield.

This paper presents compact SPICE models for the radiated and conducted susceptibility analyses of multiconductor shielded cables. These models are derived from the transmission-line equations of multiconductor shielded cables. They do not need the discretization of shielded cables and allow the transient analysis when there are nonlinear or time-varying loads at the termination. Multiconductor shielded cables over a ground excited by an incident plane-wave electromagnetic field or a lumped current source on the shield are studied with the proposed models. The differential and common mode voltages obtained by these models agree well with those from other methods.

2. DEVELOPMENT OF SPICE MOEDLS FOR MULTICONDUCTOR SHIELDED CABLES

A shielded cable over an infinite and perfectly conducting ground, as shown in Figure 1, can be considered as two transmission line systems, when its cross section and height over the ground are electrically small

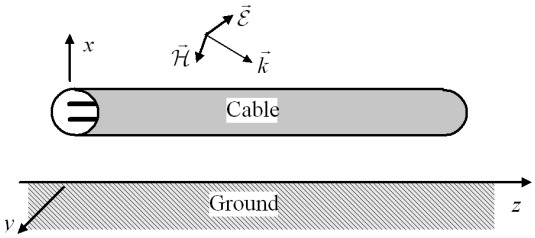

Figure 1. A multiconductor shielded cable over an infinite and perfectly conducting ground.

compared with the wavelength [15, 16]. The exterior of the shield and the ground compose the outer system, while the interior of the shield and the inner wires form the inner system. These two systems are coupled through the transfer impedance and admittance of the shield.

2.1. SPICE Models for Radiated Susceptibility Analysis

A multiconductor shielded cable with n parallel wires located inside the shield above the ground, excited by an incident plane-wave electromagnetic field, can be described by [13]

$$\frac{d}{dz}\begin{bmatrix} \hat{V}_{out} \\ \hat{\mathbf{V}}_{in} \end{bmatrix} + \begin{bmatrix} \hat{Z}_{out} & -\hat{\mathbf{Z}}_t^T \\ -\hat{\mathbf{Z}}_t & \hat{\mathbf{Z}}_{in} \end{bmatrix} \begin{bmatrix} \hat{I}_{out} \\ \hat{\mathbf{I}}_{in} \end{bmatrix} = \begin{bmatrix} \hat{V}_{sout} \\ \mathbf{0} \end{bmatrix} \tag{1a}$$

$$\frac{d}{dz}\begin{bmatrix} \hat{I}_{out} \\ \hat{\mathbf{I}}_{in} \end{bmatrix} + \begin{bmatrix} \hat{Y}_{out} & \hat{\mathbf{Y}}_t^T \\ \hat{\mathbf{Y}}_t & \hat{\mathbf{Y}}_{in} \end{bmatrix} \begin{bmatrix} \hat{V}_{out} \\ \hat{\mathbf{V}}_{in} \end{bmatrix} = \begin{bmatrix} \hat{I}_{sout} \\ \mathbf{0} \end{bmatrix}, \tag{1b}$$

where $\hat{V}_{out}$ is the shield-to-ground voltage, $\hat{I}_{out}$ is the current flowing between the external shield and the ground, $\hat{\mathbf{V}}_{in} = \left[\hat{V}_{in1}, \hat{V}_{in2}, \cdots, \hat{V}_{inn}\right]^T$ is the inner voltage vector whose kth element $\hat{V}_{ink}$ is the voltage of the kth wire versus the internal part of the shield, and $\hat{\mathbf{I}}_{in} = \left[\hat{I}_{in1}, \hat{I}_{in2}, \cdots, \hat{I}_{inn}\right]^T$ is the inner current vector whose kth element $\hat{I}_{ink}$ is the current of the kth wire. $\hat{Z}_{out}$ and $\hat{Y}_{out}$ are the per-unit-length (p.u.l.) impedance and admittance of the outer system, respectively. $\hat{\mathbf{Z}}_t = \left[\hat{Z}_{t1}, \cdots, \hat{Z}_{tn}\right]^T$ is the transfer impedance vector whose kth element $\hat{Z}_{tk}$ is the shield transfer impedance relative to the kth wire, while $\hat{\mathbf{Y}}_t = \left[\hat{Y}_{t1}, \cdots, \hat{Y}_{tn}\right]^T$ the transfer admittance vector of which kth element $\hat{Y}_{tk}$ refers to the shield transfer admittance relative to the the kth wire. The submatrices $\hat{\mathbf{Z}}_{in}$ and $\hat{\mathbf{Y}}_{in}$ are the p.u.l. impedance and admittance matrices of the inner system, respectively. $\hat{V}_{s\,out}$ and $\hat{I}_{s\,out}$ are the distributed voltage and current sources of the outer system, respectively, generated by the incident electromagnetic field [17, 18].

For the sake of simplicity, some assumptions are made. These assumptions are: 1) the loss of the multiconductor shielded cable is neglected, which may be not reasonable when the cable is extremely long and the frequency is very high [19], but ensures the worst case condition; 2) the energy transferred from the inner system to the outer system through the shield is neglected, which implies the good shielding approximation; 3) the transfer impedance $\hat{Z}_{tk}$ $(k = 1, \ldots, n)$ is taken

as $\hat{Z}_{tk}(\omega) = R_{dck} + j\omega L_{tk}$ where R_{dck} is the constant p.u.l. transfer resistance of the shield relative to the kth wire, which is greater than its true value but the worst case is considered [11], and L_{tk} is the p.u.l. transfer inductance of the shield relative to the kth wire. Under these assumptions, Equation (1) can be written as

$$\frac{d}{dz}\hat{V}_{out} + j\omega L_{out}\hat{I}_{out} = \hat{V}_{sout} \tag{2a}$$

$$\frac{d}{dz}\hat{I}_{out} + j\omega C_{out}\hat{V}_{out} = \hat{I}_{sout} \tag{2b}$$

$$\frac{d}{dz}\hat{\mathbf{V}}_{in} + j\omega \mathbf{L}_{in}\hat{\mathbf{I}}_{in} = \hat{\mathbf{Z}}_t\hat{I}_{out} \tag{2c}$$

$$\frac{d}{dz}\hat{\mathbf{I}}_{in} + j\omega \mathbf{C}_{in}\hat{\mathbf{V}}_{in} = -\hat{\mathbf{Y}}_t\hat{V}_{out}, \tag{2d}$$

where L_{out} and C_{out} are the p.u.l inductance and capacitance of the outer system, respectively, while $\mathbf{L}_{in}$ and $\mathbf{C}_{in}$ the p.u.l inductance and capacitance matrices of the inner system.

The responses of the outer loads can be obtained with some already developed SPICE models [1, 2], so the solutions to the response of the inner loads are the interest of this paper. Equations (2c) and (2d) can be decoupled with a similarity transformation. Define the transformation to mode quantities as

$$\hat{\mathbf{V}}_{in} = \mathbf{T}_V\hat{\mathbf{V}}_{inm} \tag{3a}$$

$$\hat{\mathbf{I}}_{in} = \mathbf{T}_I\hat{\mathbf{I}}_{inm}. \tag{3b}$$

Substituting (3) into (2c) and (2d) gives

$$\frac{d}{dz}\hat{\mathbf{V}}_{inm} + j\omega \mathbf{L}_{inm}\hat{\mathbf{I}}_{inm} = \hat{\mathbf{V}}_{Finm} \tag{4a}$$

$$\frac{d}{dz}\hat{\mathbf{I}}_{inm} + j\omega \mathbf{C}_{inm}\hat{\mathbf{V}}_{inm} = \hat{\mathbf{I}}_{Finm}, \tag{4b}$$

where

$$\mathbf{L}_{inm} = \mathbf{T}_V^{-1}\mathbf{L}_{in}\mathbf{T}_I \tag{5a}$$

$$\mathbf{C}_{inm} = \mathbf{T}_I^{-1}\mathbf{C}_{in}\mathbf{T}_V \tag{5b}$$

$$\hat{\mathbf{V}}_{Finm} = \mathbf{T}_V^{-1}\hat{\mathbf{Z}}_t\hat{I}_{out} \tag{5c}$$

$$\hat{\mathbf{I}}_{Finm} = -\mathbf{T}_I^{-1}\hat{\mathbf{Y}}_t\hat{V}_{out}. \tag{5d}$$

Both $\mathbf{L}_{inm}$ and $\mathbf{C}_{inm}$ are diagonal matrices, and the matrices $\mathbf{T}_V$ and $\mathbf{T}_I$ are frequency independent when the loss is neglected. From (4), the relation between the terminal mode voltages and currents can be

written as

$$\begin{aligned} & \hat{\mathbf{V}}_{inm}(0) - \mathbf{Z}_{Cinm}\hat{\mathbf{I}}_{inm}(0) \\ = \; & e^{-j\omega\mathbf{\Lambda}\mathcal{L}}\left[\hat{\mathbf{V}}_{inm}(\mathcal{L}) - \mathbf{Z}_{Cinm}\hat{\mathbf{I}}_{inm}(\mathcal{L})\right] + \hat{\mathbf{V}}_{0inm} \qquad (6a) \\ & \hat{\mathbf{V}}_{inm}(\mathcal{L}) + \mathbf{Z}_{Cinm}\hat{\mathbf{I}}_{inm}(\mathcal{L}) \\ = \; & e^{-j\omega\mathbf{\Lambda}\mathcal{L}}\left[\hat{\mathbf{V}}_{inm}(0) + \mathbf{Z}_{Cinm}\hat{\mathbf{I}}_{inm}(0)\right] + \hat{\mathbf{V}}_{\mathcal{L}inm}, \qquad (6b) \end{aligned}$$

where $\mathcal{L}$ is the length of the cable, $\mathbf{Z}_{Cinm}$ is the mode characteristic impedance diagonal matrix of the inner system, and $\mathbf{\Lambda}$ is a diagonal matrix defined by $\mathbf{\Lambda} = \sqrt{\mathbf{L}_{inm}\mathbf{C}_{inm}}$. $\hat{\mathbf{V}}_{0inm}$ and $\hat{\mathbf{V}}_{\mathcal{L}inm}$ are the effect of the distributed source of the inner system, given by

$$\begin{aligned} \hat{\mathbf{V}}_{0inm} = & -\int_0^{\mathcal{L}} e^{-j\beta_{in}z} \\ & \left\{\mathbf{R}_{dc}^{eq} I_{out}(z) + j\omega\left[\mathbf{L}_t^{eq} I_{out}(z) + \mathbf{Z}_{Cinm}\mathbf{C}_t^{eq} V_{out}(z)\right]\right\} dz \qquad (7a) \\ \hat{\mathbf{V}}_{\mathcal{L}inm} = & \int_0^{\mathcal{L}} e^{-j\beta_{in}(\mathcal{L}-z)} \\ & \left\{\mathbf{R}_{dc}^{eq} I_{out}(z) + j\omega\left[\mathbf{L}_t^{eq} I_{out}(z) - \mathbf{Z}_{Cinm}\mathbf{C}_t^{eq} V_{out}(z)\right]\right\} dz, \qquad (7b) \end{aligned}$$

where

$$\begin{aligned} \beta_{in} &= \omega\mathbf{\Lambda} && (8a) \\ \mathbf{R}_{dc}^{eq} &= \mathbf{T}_V^{-1}\mathbf{R}_{dc} && (8b) \\ \mathbf{L}_t^{eq} &= \mathbf{T}_V^{-1}\mathbf{L}_t && (8c) \\ \mathbf{C}_t^{eq} &= \mathbf{T}_I^{-1}\mathbf{C}_t. && (8d) \end{aligned}$$

Equation (6) can be considered as n independent single-wire transmission lines, and each element can be written in the time domain as

$$\begin{aligned} & \left[\mathbf{V}_{inm}(0,t) - \mathbf{Z}_{Cinm}\mathbf{I}_{inm}(0,t)\right]_i \\ = \; & \left[\mathbf{V}_{inm}(\mathcal{L},t-T_i) - \mathbf{Z}_{Cinm}\mathbf{I}_{inm}(\mathcal{L},t-T_i)\right]_i + \left[\mathbf{V}_{0in}(t)\right]_i \qquad (9a) \\ & \left[\mathbf{V}_{inm}(\mathcal{L},t) + \mathbf{Z}_{Cinm}\mathbf{I}_{inm}(\mathcal{L},t)\right]_i \\ = \; & \left[\mathbf{V}_{inm}(0,t-T_i) + \mathbf{Z}_{Cinm}\mathbf{I}_{inm}(0,t-T_i)\right]_i + \left[\mathbf{V}_{\mathcal{L}in}(t)\right]_i, \qquad (9b) \end{aligned}$$

where T_i is the one-way delay of the ith mode line. The elements of $\hat{\mathbf{V}}_{0inm}$ and $\hat{\mathbf{V}}_{\mathcal{L}inm}$ are similar to those of the coaxial cable, so $\left[\mathbf{V}_{0in}(t)\right]_i$ and $\left[\mathbf{V}_{\mathcal{L}in}(t)\right]_i$ can be written as [14]

$$\begin{aligned} \left[\mathbf{V}_{0in}(t)\right]_i = & -\frac{1}{2Z_{Cout}}\left(\left[\mathbf{R}_{dc}^{eq}\right]_i + B_i\frac{d}{dt}\right)E_{i1}(t) \\ & +\frac{1}{2Z_{Cout}}\left(\left[\mathbf{R}_{dc}^{eq}\right]_i + C_i\frac{d}{dt}\right)E_{i2}(t) \qquad (10a) \end{aligned}$$

$$[\mathbf{V}_{\mathcal{L}in}(t)]_i = \frac{1}{2Z_{Cout}}\left([\mathbf{R}_{dc}^{eq}]_i + C_i\frac{d}{dt}\right)E_{i3}(t) - \frac{1}{2Z_{Cout}}\left([\mathbf{R}_{dc}^{eq}]_i + B_i\frac{d}{dt}\right)E_{i4}(t), \quad (10b)$$

where the coefficients B_i and C_i are given by

$$B_i = [\mathbf{L}_t^{eq}]_i + Z_{Cout}[\mathbf{Z}_{Cin\,m}]_i[\mathbf{C}_t^{eq}]_i \quad (11a)$$

$$C_i = [\mathbf{L}_t^{eq}]_i - Z_{Cout}[\mathbf{Z}_{Cin\,m}]_i[\mathbf{C}_t^{eq}]_i, \quad (11b)$$

and the voltages E_{ik} $(k = 1, \ldots, 4)$ is composed of two parts $E_{tik}(t)$ and $E_{sik}(t)$. $E_{tik}(t)$ $(k = 1, \ldots, 4)$ are the outer system's terminal voltage and current's contribution to E_{ik}, and are given by [14]

$$E_{tik}(t) = \int_{-\infty}^{t} F_{tik}(t')\,dt', \quad k = 1, \ldots, 4 \quad (12)$$

where

$$F_{ti1}(t) = \frac{\mathcal{L}}{T_i + T_{out}}\{[V_{out}(0,t) + Z_{Cout}I_{out}(0,t)] - [V_{out}(0,t-T_i-T_{out}) + Z_{Cout}I_{out}(0,t-T_i-T_{out})]\} \quad (13a)$$

$$F_{ti2}(t) = \frac{\mathcal{L}}{T_{out} - T_i}\{[V_{out}(\mathcal{L},t-T_i) - Z_{Cout}I_{out}(\mathcal{L},t-T_i)] - [V_{out}(\mathcal{L},t-T_{out}) - Z_{Cout}I_{out}(\mathcal{L},t-T_{out})]\} \quad (13b)$$

$$F_{ti3}(t) = \frac{\mathcal{L}}{T_{out} - T_i}\{[V_{out}(0,t-T_i) + Z_{Cout}I_{out}(0,t-T_i)] - [V_{out}(0,t-T_{out}) + Z_{Cout}I_{out}(0,t-T_{out})]\} \quad (13c)$$

$$F_{ti4}(t) = \frac{\mathcal{L}}{T_i + T_{out}}\{[V_{out}(\mathcal{L},t) - Z_{Cout}I_{out}(\mathcal{L},t)] - [V_{out}(\mathcal{L},t-T_i-T_{out}) - Z_{Cout}I_{out}(\mathcal{L},t-T_i-T_{out})]\}. \quad (13d)$$

Here T_{out} is the one-way delay of the outer system. Thus the voltage E_{tik} $(k = 1, \ldots, 4)$ can be realized through integral circuits, delay lines and controlled sources. When $T_i = T_{out}$, (13b) and (13c) seem to be undefined, however, they can be realized by differential circuits. $E_{sik}(t)$ $(k = 1, \ldots, 4)$ are the contributions related to external fields. When the incident electromagnetic field is a plane wave, and its incident direction and polarization are defined as in [1, 2], $E_{sik}(t)$ $(k = 1, \ldots, 4)$ can be written as [14]

$$E_{sik}(t) = \int_{-\infty}^{t} F_{sik}(t')\,dt', \quad k = 1, \ldots, 4 \quad (14)$$

where

$$F_{si1}(t) = 2h\mathcal{L}\frac{e_xT_z - e_zT_x - e_xT_{out}}{T_z - T_{out}} \left\{\frac{\mathcal{E}_0(t) - \mathcal{E}_0(t - T_i - T_{out})}{T_{out} + T_i} - \frac{\mathcal{E}_0(t) - \mathcal{E}_0(t - T_z - T_i)}{T_z + T_i}\right\} \quad (15a)$$

$$F_{si2}(t) = -2h\mathcal{L}\frac{e_xT_z - e_zT_x + e_xT_{out}}{T_z + T_{out}} \left\{\frac{\mathcal{E}_0(t) - \mathcal{E}_0(t - T_z - T_i)}{T_z + T_i} + \frac{\mathcal{E}_0(t - T_z - T_i) - \mathcal{E}_0(t - T_z - T_{out})}{T_i - T_{out}}\right\} \quad (15b)$$

$$F_{si3}(t) = 2h\mathcal{L}\frac{e_xT_z - e_zT_x - e_xT_{out}}{T_z - T_{out}} \left\{\frac{\mathcal{E}_0(t - T_z) - \mathcal{E}_0(t - T_i)}{T_z - T_i} - \frac{\mathcal{E}_0(t - T_i) - \mathcal{E}_0(t - T_{out})}{T_i - T_{out}}\right\} \quad (15c)$$

$$F_{si4}(t) = 2h\mathcal{L}\frac{e_xT_z - e_zT_x + e_xT_{out}}{T_z + T_{out}} \left\{\frac{\mathcal{E}_0(t - T_z) - \mathcal{E}_0(t - T_i)}{T_z - T_i} + \frac{\mathcal{E}_0(t - T_z) - \mathcal{E}_0(t - T_z - T_i - T_{out})}{T_i + T_{out}}\right\}. \quad (15d)$$

Here h is the height of the cable over the ground, $\mathcal{E}_0$ is the expression for the electric field, e_x and e_z are the x and z components of the incident electric field vector, and T_x and T_z are defined as $T_x = \mathcal{L}/v_x$ and $T_z = \mathcal{L}/v_z$, where v_x and v_z are the velocities of the wave propagation along the x and z axes. According to (14) and (15), $E_{sik}(t)$ $(k = 1, \ldots, 4)$ can be realized through integral circuits, delay lines, controlled sources, and differential circuits when they are needed.

To allow loads to be connected between the inner wires and the ground, the transformation of the voltages and currents of the outer and inner systems to the voltages (referenced to ground) and currents of the shield and the wires is needed [10], which are denoted by $V_0, V_1, \ldots, V_n$, and $I_0, I_1, \ldots, I_n$. With (3), the transformation can be written as

$$\begin{bmatrix} \hat{V}_0 \\ \hat{\mathbf{V}}_{\mathrm{I}} \end{bmatrix} = \begin{bmatrix} 1 & \mathbf{0}^T \\ \mathbf{1} & \mathbf{T}_V \end{bmatrix} \begin{bmatrix} \hat{V}_{out} \\ \hat{\mathbf{V}}_{inm} \end{bmatrix} \quad (16a)$$

$$\begin{bmatrix} \hat{I}_{out} \\ \hat{\mathbf{I}}_{inm} \end{bmatrix} = \begin{bmatrix} 1 & \mathbf{1}^T \\ \mathbf{0} & \mathbf{T}_I^{-1} \end{bmatrix} \begin{bmatrix} \hat{I}_0 \\ \hat{\mathbf{I}}_{\mathrm{I}} \end{bmatrix}, \quad (16b)$$

where $\hat{\mathbf{V}}_{\mathrm{I}} = [V_1, \cdots, V_n]^T$, $\hat{\mathbf{I}}_{\mathrm{I}} = [I_1, \cdots, I_n]^T$, $\mathbf{0}$ is a $n \times 1$ vector with each element equals 0, and $\mathbf{1}$ is a $n \times 1$ vector whose elements are 1. Equation (16) can be realized in SPICE by using controlled sources.

It should be noted that the responses obtained by this model should be divided by 2 when the wave propagates parallelly to the ground [14].

The SPICE circuit for a multiconductor shielded cable excited by an incident plane-wave electromagnetic field is shown in Figure 2, where R_1 and R_2 are large resistances (like 1GΩ) to avoid floating nodes according to the SPICE syntax. The controlled voltage sources E_{0out}, $E_{\Lambda out}$, E_{i0}, and $E_{i\Lambda}$, are given by

$$
\begin{aligned}
E_{0out}(t) &= -2h\left(e_x - e_z T_x/(T_z + T_{out})\right)\left[V(400) - V(403)\right] \\
E_{\mathcal{L}out}(t) &= \begin{cases} 2h\left(e_x - e_z T_x/T_z - T_{out}\right)\left[V(401) - V(402)\right] & (Tz \neq T_{out}) \\ 0 & (Tz = T_{out}) \end{cases} \\
E_{i0} &= \frac{1}{2Z_{Cout}}\left\{\left[\mathbf{R}_{dc}^{eq}\right]_i \left[V(i321, i322) - V(i311, i312)\right]\right. \\
&\quad \left. -B_i V(i312) + C_i V(i322)\right\} \\
E_{i\mathcal{L}} &= \frac{1}{2Z_{Cout}}\left\{\left[\mathbf{R}_{dc}^{eq}\right]_i \left[V(i331, i332) - V(i341, i342)\right]\right. \\
&\quad \left. -B_i V(i342) + C_i V(i332)\right\}
\end{aligned}
$$

2.2. SPICE Models for Conducted Susceptibility Analysis

The development of the SPICE model for conducted susceptibility analysis is similar to and much simpler than that for radiated susceptibility analysis. This model can be easily obtained by setting $\hat{V}_{s\,out}$ and $\hat{I}_{s\,out}$ to zero, and modeling the excitation with a lumped source at the end of the cable. The SPICE circuit for conducted susceptibility analysis can be realized by removing the controlled sources E_{0out}, $E_{\mathcal{L}out}$, F_{sik}, and their realization circuits in Figure 2.

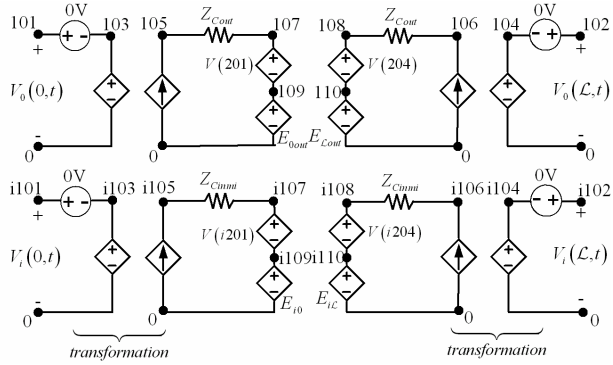

(a)

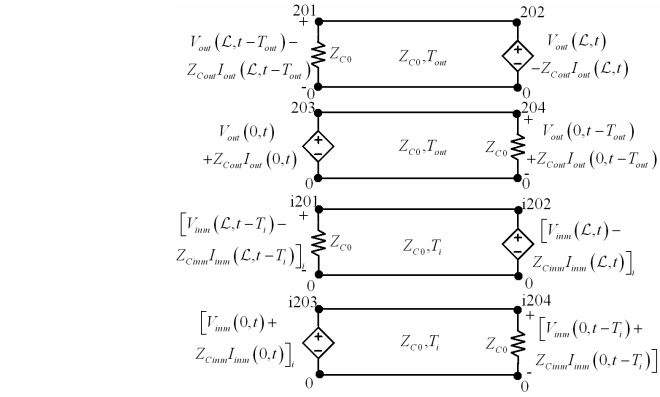

(b)

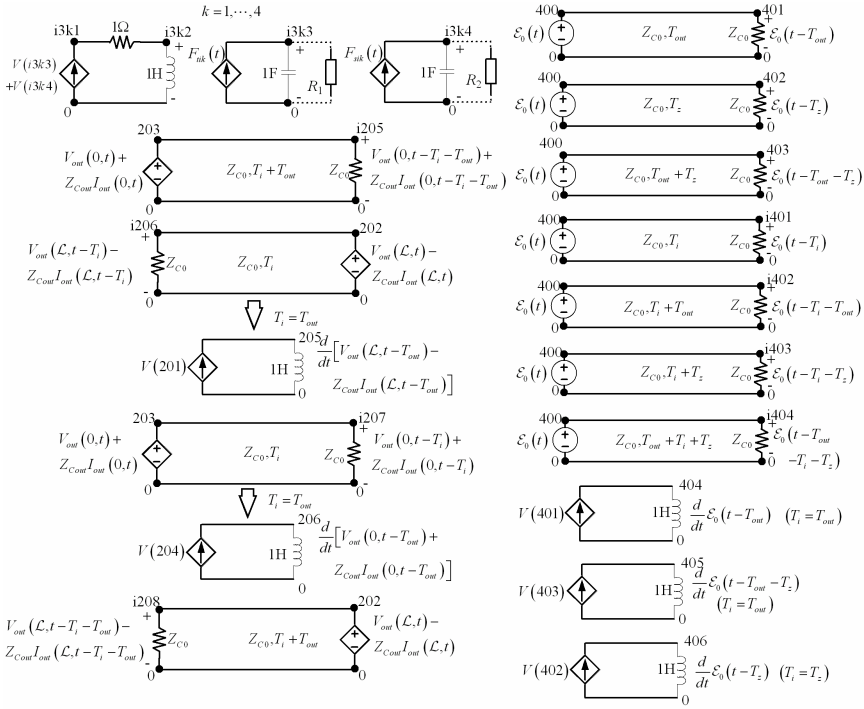

(c)

Figure 2. The SPICE circuit for multiconductor shielded cables excited by an incident plane-wave electromagnetic field. (a) The main circuit. (b) The realization circuits of the controlled voltage sources $V(201)$, $V(204)$, $V(i201)$, and $V(i204)$. (c) The realization circuits of the controlled sources E_{0out}, $E_{\mathcal{L}out}$, E_{i0}, and $E_{i\mathcal{L}}$.

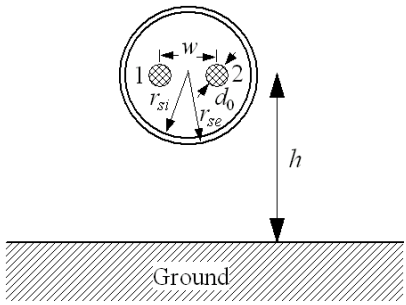

Figure 3. The cross section of a two-parallel-wire shielded cable.

Table 1. Parameters of the shield.

C	P (mm^{-1})	N	d (mm)	α (degree)
16	0.17	12	0.18	27.6

3. NUMERICAL VALIDATIONS OF SPICE MODELS

The analysis is carried out on a two-parallel-wire shielded cable as shown in Figure 3. The outer radius r_{se} and the inner radius r_{si} of the braided shield are 7.49 mm and 7.13 mm, respectively. The characteristics of the braided shield can be defined in terms of the number of carriers C, the picks P, the ends N, the wire diameter d, and the weave angle α [15, 16]. The values of these parameters are given in Table 1. The two inner wires with the diameter $d_0 = 2\,\mathrm{mm}$ and the distance $w = 5.64\,\mathrm{mm}$ are located symmetrically.

The differential and common mode disturbances at the termination due to a plane-wave electromagnetic field or a lumped current source are computed. The differential voltages V_{DMi} $(i = 1, 2)$ are the voltages across the resistances R_{Di} $(i = 1, 2)$, and the common mode voltages V_{CMi} $(i = 1, 2)$ are defined as

$$V_{\mathrm{CM\,i}} = (I_{i1} + I_{i2}) \frac{R_{i1} R_{i2}}{R_{i1} + R_{i2}} \quad (i = 1, 2)\,, \tag{17}$$

where I_{i1} and I_{i2} are the current through R_{i1} and R_{i2}, and their positive direction is defined as the direction towards the loads.

3.1. Radiated Susceptibility Analysis

In the radiated susceptibility analysis, an incident electromagnetic wave with its electric field modeled by a biexponential pulse $\mathcal{E}_0(t) = kE_0 [\exp(-\beta t) - \exp(-\alpha t)]$, where $k = 1.3$, $E_0 = 50\,\mathrm{kV/m}$, $\alpha =$

$6.0e8\,\mathrm{s}^{-1}$, and $\beta = 4.0e7\,\mathrm{s}^{-1}$, is used for the time domain analysis, while the electric field of $1\,\mathrm{V/m}$ magnitude for the frequency domain analysis.

The first configuration for the radiated susceptibility analysis is shown in Figure 4, where the shield is grounded at both ends (e.g., $R_1 = R_2 = 0$), R_{11}, R_{12}, and R_{D1} are $200\,\Omega$, $50\,\Omega$, and $100\,\Omega$, respectively, and the loads at the right termination has the same value as those at the left end. The length and height of the cable are 3 m and 2 cm, respectively. The incident wave propagates perpendicularly to the ground with the electric field parallel to the z axis. Figure 5 and Figure 6 show the differential and common mode voltages in the time and frequency domain analyses, respectively, where "multiconductor" means the multiconductor method [20] in which (1) is solved and the assumptions mentioned above have not been adopted,

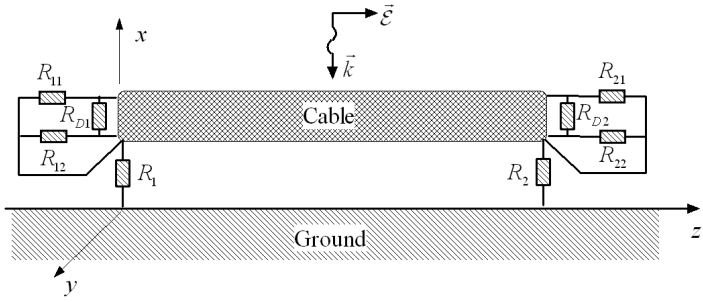

Figure 4. The configuration for the radiated analysis.

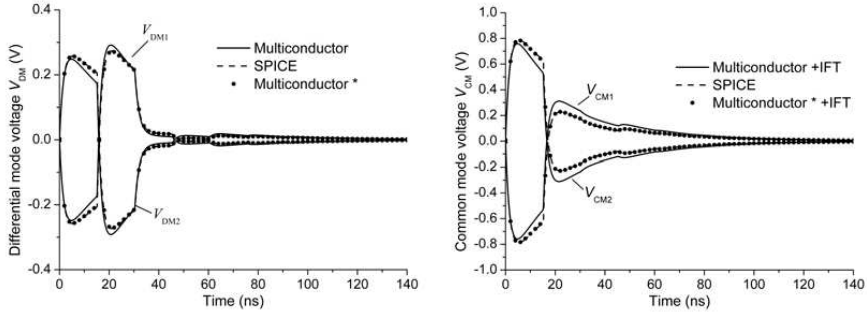

Figure 5. The disturbances at the cable ends in the time domain analysis with the incident wave propagating in the $-x$ direction. (a) Differential mode voltages. (b) Common mode voltages.

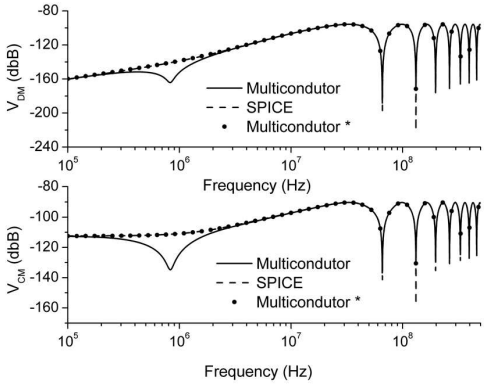

Figure 6. The disturbances at the cable ends in the frequency domain analysis with the incident wave propagating in the $-x$ direction.

and "multiconductor *" means the multiconductor method but with the assumption $\hat{Z}_{tk}(\omega) = R_{dck} + j\omega L_{tk}$ $(k = 1, \ldots, n)$ used. The results show that the voltages at the two ends have the same size but opposite polarity, and the differences between the results from the SPICE model and the multiconductor method are primarily due to the assumption $\hat{Z}_{tk}(\omega) = R_{dck} + j\omega L_{tk}$ $(k = 1, \ldots, n)$.

The second configuration considered is similar to the first one but with the incident wave propagating along the z axis, the electric field parallel to the x axis, and R_{21}, R_{22}, and R_{D2} set to $1\,\mathrm{G}\Omega$, $0\,\Omega$, and $1\,\mathrm{G}\Omega$, respectively. As mentioned above, the SPICE model can also be used when the loads are nonlinear. Thus, a voltage clipper, which is formed by two anti-parallel 1N4148 diodes, is added to the right termination and is in parallel with the load R_{D2} in this configuration. Figure 7 and Figure 8 show the differential and common mode voltages at the cable ends in presence and in absence of the voltage clipper, respectively. But only the common mode voltage V_{CM} at the left termination is given, because the right end is grounded, namely, $R_{22} = 0\,\Omega$. The differences of the curves in presence and in absence of the voltage clipper reveal the effects of the nonlinear device, which depresses the differential mode voltages and increases the common mode voltage.

3.2. Conducted Susceptibility Analysis

The configuration used for the conducted susceptibility analysis is shown in Figure 9, where a lumped current source is connected to

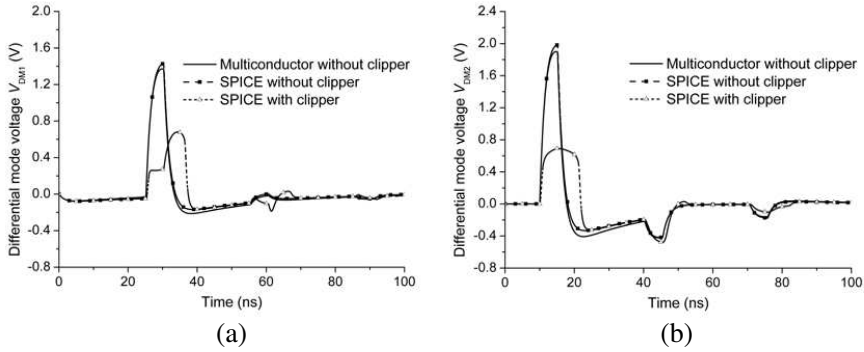

Figure 7. The differential mode voltage induced by the incident wave in presence and in absence of the voltage clipper. (a) The differential mode voltage V_{DM1} at the left termination. (b) The differential mode voltage V_{DM2} at the right termination.

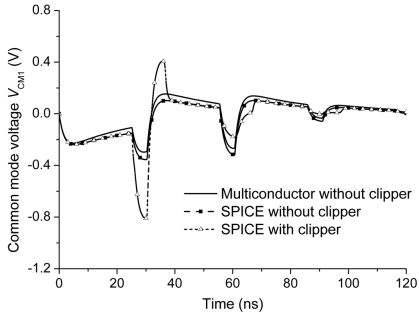

Figure 8. The common mode voltage V_{CM1} induced by the incident wave at the left termination.

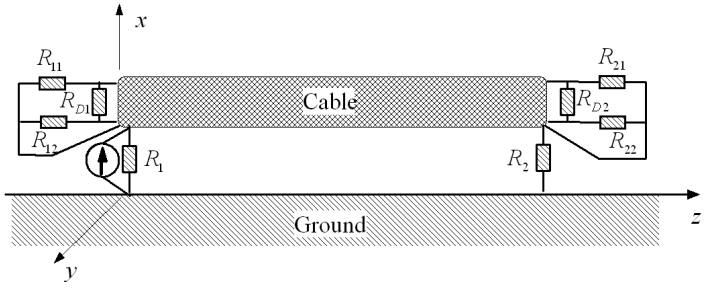

Figure 9. The configuration for the conducted susceptibility analysis.

the cable shield at the left end. The length and the height of the cable are set to 5 m and 3 cm, respectively. In this configuration, the inner loads $R_{D1} = \infty$, $R_{12} = \infty$, and $R_{11} = 0$. The outer load R_1 equals to the characteristic impedance of the outer system. The loads at the right end have same value as those at the left end. Other parameters of the cable are the same as those in the radiated susceptibility analysis.

The current source adopted for the time domain analysis is a clock wave of unit amplitude characterized by period $T_{clk} = 20$ ns, rise and fall time $T_r = T_f = 1$ ns, and duty cycle $\eta = 0.5$, while a AC current source of 1 A for the frequency domain analysis. The outer terminal voltages and the differential mode voltages obtained by the proposed

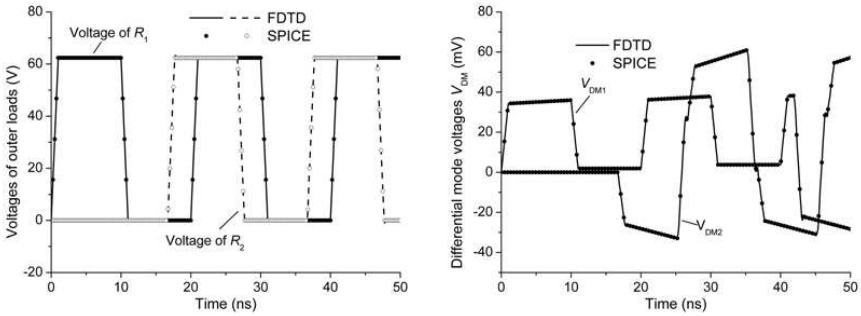

Figure 10. The responses obtained in the time domain analysis. (a) The voltages of the outer termination. (b) The differential mode voltages at the cable ends.

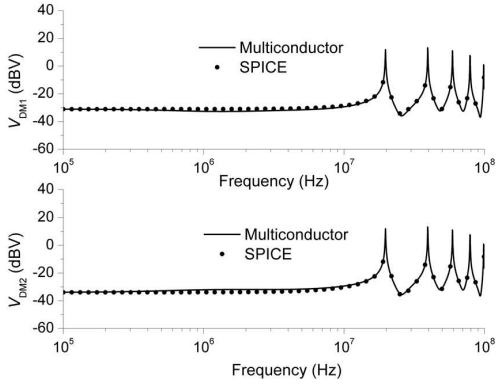

Figure 11. The voltage responses in the frequency domain analysis.

model in the time domain analysis are shown in Figure 10, where the "FDTD" means the finite difference time domain solution to the transmission-line equations of the cable. The differential mode voltages in the frequency domain analysis are shown in Figure 11. The results show that the solutions from different methods are in good agreement.

4. SUMMARY AND CONCLUSION

Compact SPICE models for the radiated and conducted susceptibility analyses of multiconductor shielded cables in the time and frequency domains have been proposed, and their numerical validations have been given. Based on the four main assumptions: 1) multiconductor shielded cables are lossless; 2) the energy transferred from the inner to the outer system can be neglected; 3) the resistance part of the transfer impedance is frequency independent; 4) the height of cables over the ground is electrically small, the proposed models are derived from the transmission-line equations of multiconductor shielded cables. These SPICE models do not need any discretization of cables and allow the transient analysis when there are nonlinear or time-varying loads at the termination. Results obtained by these models agree well with those from other methods.

ACKNOWLEDGMENT

Acknowledgement is made to National Natural Science Foundation of China for the support of this research through Grant No. 60971080.

REFERENCES

1. Paul, C. R., "A SPICE model for multiconductor transmission lines excited by an incident electromagnetic field," *IEEE Trans. Electromagn. Compat.*, Vol. 36, No. 4, 342–354, 1994.
2. Paul, C. R., *Analysis of Multiconductor Transmission Lines*, 417–418, Wiley, New York, 1994.
3. Celozz, S. and M. Feliziani, "Time-domain solution of field-excited multiconductor transmission line equations," *IEEE Trans. Electromagn. Compat.*, Vol. 37, No. 3, 421–432, 1995.
4. Maio, I., F. G. Canavero, and B. Dilecce, "Analysis of crosstalk and field coupling to lossy MTLs in a SPICE environment," *IEEE Trans. Electromagn. Compat.*, Vol. 38, No. 3, 221–229, 1996.

5. Erdin, I., A. Dounavis, R. Achar, et al., "A SPICE model for incident field coupling to lossy multiconductor transmission lines," *IEEE Trans. Electromagn. Compat.*, Vol. 43, No. 4, 485–494, 2001.
6. Erdin, I., A. Dounavis, R. Achar, et al., "Circuit simulation of incident field coupling to multiconductor transmission lines with frequency-dependent losses," *Proc. IEEE Int. Symp. Electromagnetic Compatibility*, Vol. 2, 1084–1087, 2001
7. Xie, H., J. Wang, R. Fan, et al., "A hybrid FDTD-SPICE method for transmission lines excited by a nonuniform incident wave," *IEEE Trans. Electromagn. Compat.*, Vol. 51, No. 3, 811–817, 2009.
8. Xie, H., J. Wang, D. Sun, R. Fan, and Y. Liu, "SPICE simulation and experimental study of transmission lines with TVSs excited by EMP," *Journal of Electromagnetic Waves and Applications*, Vol. 24, No. 2–3, 401–411, 2010.
9. Xie, H., J. Wang, D. Sun, R. Fan, and Y. Liu, "Analysis of EMP coupling to a device from a wire penetrating a cavity aperture using transient electromagnetic topology," *Journal of Electromagnetic Waves and Applications*, Vol. 23, No. 17–18, 2313–2322, 2009.
10. Caniggia, S. and F. Maradei, "Equivalent circuit models for the analysis of coaxial cables immunity," *Proc. IEEE Int. Symp. Electromagnetic Compatibility*, Vol. 2, 881–886, 2003.
11. Orlandi, A., "Circuit model for bulk current injection test on shielded coaxial cables," *IEEE Trans. Electromagn. Compat.*, Vol. 45, No. 4, 602–615, 2003.
12. Antonini, G. and A. Orlandi, "Spice equivalent circuit of a two-parallel-wires shielded cable for evaluation of the RF induced voltages at the terminations," *IEEE Trans. Electromagn. Compat.*, Vol. 46, No. 2, 189–198, 2004.
13. Caniggia, S. and F. Maradei, "SPICE-like models for the analysis of the conducted and radiated immunity of shielded cables," *IEEE Trans. Electromagn. Compat.*, Vol. 46, No. 4, 606–616, 2004.
14. Xie, H., J. Wang, R. Fan, et al., "SPICE models to analyze radiated and conducted susceptibilities of shielded coaxial cables," *IEEE Trans. Electromagn. Compat.*, Vol. 52, No. 1, 215–222, 2010.
15. Vance, E. F., *Coupling to Shielded Cables*, Wiley, New York, 1978.
16. Tesche, F. M., M. V. Ianoz, and T. Karlsson, *EMC Analysis Methods and Computational Models*, 451–455, Wiley, New York, 1997.
17. Taylor, C. D., R. S. Satterwhite, and C. W. Harrison, "The response of a terminated two-wire transmission line excited by

a nonuniform electromagnetic field," *IEEE Trans. Antennas Propag.*, Vol. 13, No. 6, 987–989, 1965.

18. Agrawal, A. K., H. J. Price, and S. H. Gurbaxani, "Transient response of multiconductor transmission lines excited by a nonuniform electromagnetic field," *IEEE Trans. Electromagn. Compat.*, Vol. 22, No. 2, 119–129, 1980.
19. Xie, H., J. Wang, R. Fan, and Y. Liu, "Study of loss effect of transmission lines and validity of a Spice model in electromagnetic topology," *Progress In Electromagnetics Research*, PIER 90, 89–103, 2009.
20. D'Amore, M. and M. Feliziani, "EMP coupling to coaxial shielded cables," *Rec. IEEE Int. Symp. Electromagnetic Compatibility*, 37–44, 1988.